Supporting Information

Long-range charge transport in diazonium-based single-molecule junctions

Xinlei Yao[a], Xiaonan Sun[a], Frédéric Lafolet[a], Jean-Christophe Lacroix[a]**

[a] Université de Paris, ITODYS, CNRS UMR 7086, 15 rue Jean-Antoine de Baïf, 75205 Paris Cedex 13, France.

* corresponding authors

Email: sun.xiaonan@univ-paris-diderot.fr, lacroix@univ-paris-diderot.fr

1.Electrochemical data in solution 2

2.Electrochemical grafting.....3

3.Thickness measurements by AFM 4

4.STM-bj results 5

1. Electrochemical data in solution

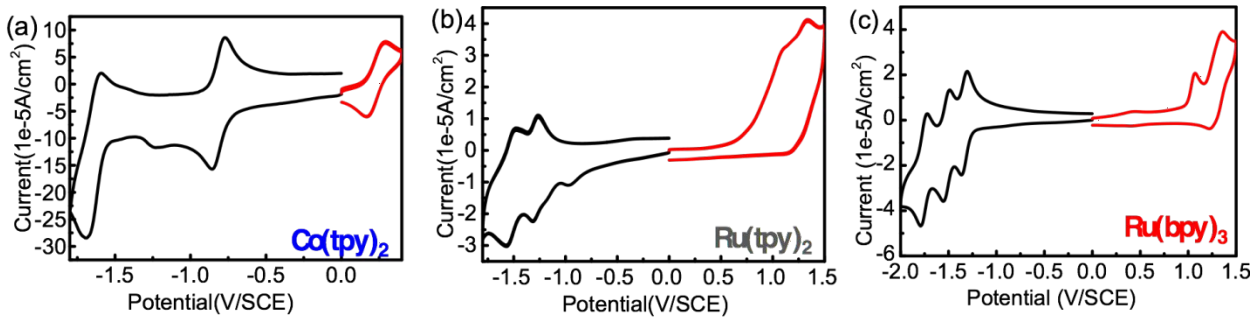

Figure S1. CV of $Co(tpy)_2$ (a), $Ru(tpy)_2$ (b), and $Ru(bpy)_3$ (c) in solution (5×10^{-4} M in ACN with 0.1 M $TBAPF_6$, scan rate 0.1 V/s) (black in negative range and red in positive range).(on glassy carbon)

2. Electrochemical grafting

$[Co(tpy)_2]_n$ Oligomers	Scan range for grafting (V/SCE)	Number of Scan cycles for grafting	Measured surface coverage Γ(mol·cm^{-2})	Most probable molecular length (nm)
n=1-2	0.4-(-0.6)	4	$(5.0\pm1.0)\times10^{-10}$	2.0
n=2-3	0.5-(-0.7)	8	$(12.5\pm1.0)\times10^{-10}$	4.0
n=3-4	0.4-(-0.7)	15	$(16.5\pm1.0)\times10^{-10}$	6.0
n=4-5	0.4-(-0.7)	24	$(22.0\pm1.0)\times10^{-10}$	8.0

Table S1. Electrochemical grafting parameters for generating $[Co(tpy)_2]_n$ oligomers on Au substrate (fabricated by e-beam evaporation on Si/SiO_2 wafers.): 5×10^{-4} M $Co(tpy)_2$ with 0.1M $TBAPF_6$ in ACN solution, scan rate 0.1V/S and peak potentials in CV of $[Co(tpy)_2]_n$ grafted on Au substrate.

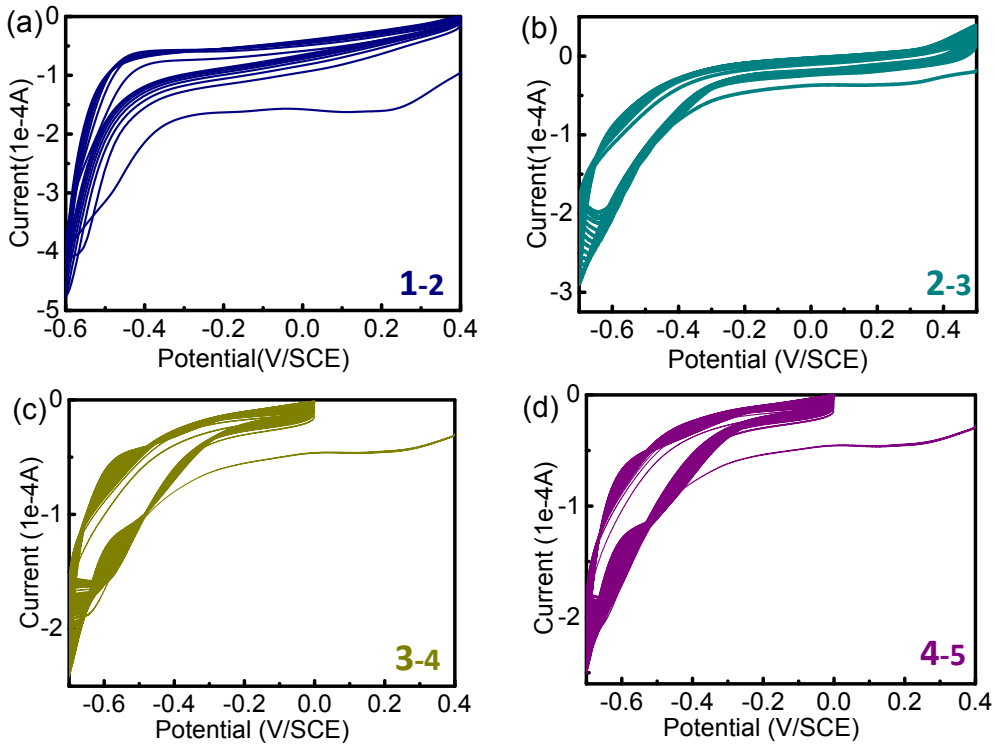

Figure S2. (a)-(d) Cyclic Voltammograms(CV) of $[Co(tpy)_2]_n$ oligomers electrografting on Au substrate with n changing from one to four. (5×10^{-4} M with 0.1M $TBAPF_6$ in ACN solution, scan rate 0.1V/S).

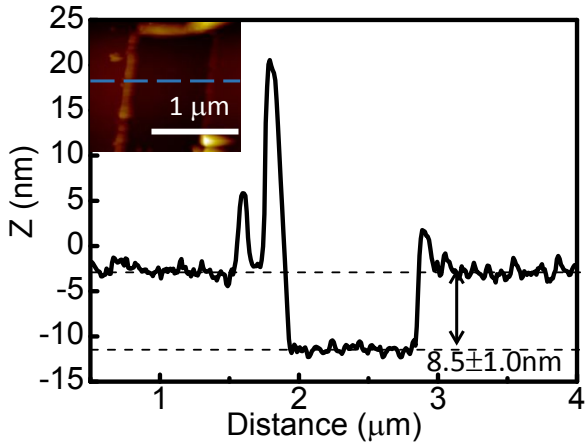

Figure S3. Thickness characterization of electrografted $[Co(tpy)_2]_n$ (n=4-5) oligomers on Au substrate by AFM scratch.

3. Thickness measurements by AFM for Ru-based layers

Molecules (Oligomers)		Scan range for grafting (V/SCE)	Number of Scan cycles for grafting	Scan rate(V/S)	AFM scratch thickness(nm)
$[Ru(tpy)_2]_n$	**n=1**-2	0.4-(-0.6)	5	0.1	2.5±1.0
	n=2-3	0-(-0.5)	15	0.1	5.0±1.0
$[Ru(bpy)_3]_n$	**n=1**-2	0.4-(-0.5)	3	0.1	2.0±1.0
	n=2-3	0.4-(-0.5)	5	0.1	3.0 ±1.0

Table S2. Electrochemical grafting parameters for $[Ru(tpy)_2]_n$ and $[Ru(bpy)_3]_n$ on Au substrate: (5×10^{-4} M with 0.1M $TBAPF_6$ in ACN solution).

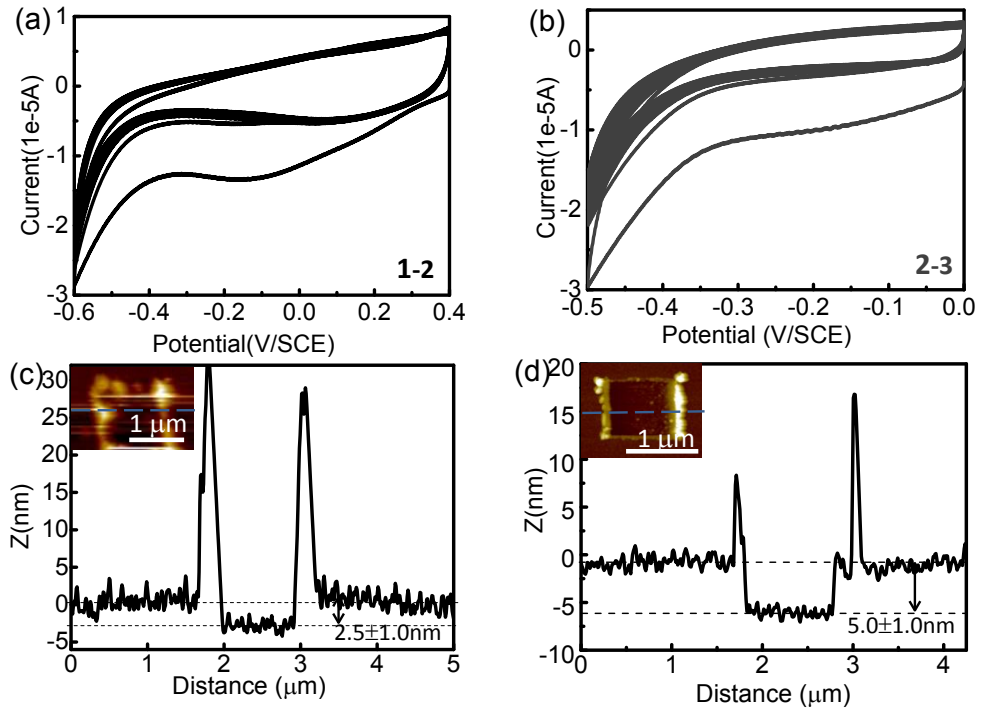

Figure S4. CV of $[Ru(tpy)_2]_n$ electrografting on Au substrate (5×10^{-4} M $Ru(tpy)_2$ with 0.1M $TBAPF_6$ in ACN solution, scan rate 0.1V/S) (a) n=1-2 (b) n=2-3.(possible type of oligomers existing on substrates) Thickness characterization by AFM scratch (c) n=1-2 (d) n=2-3.

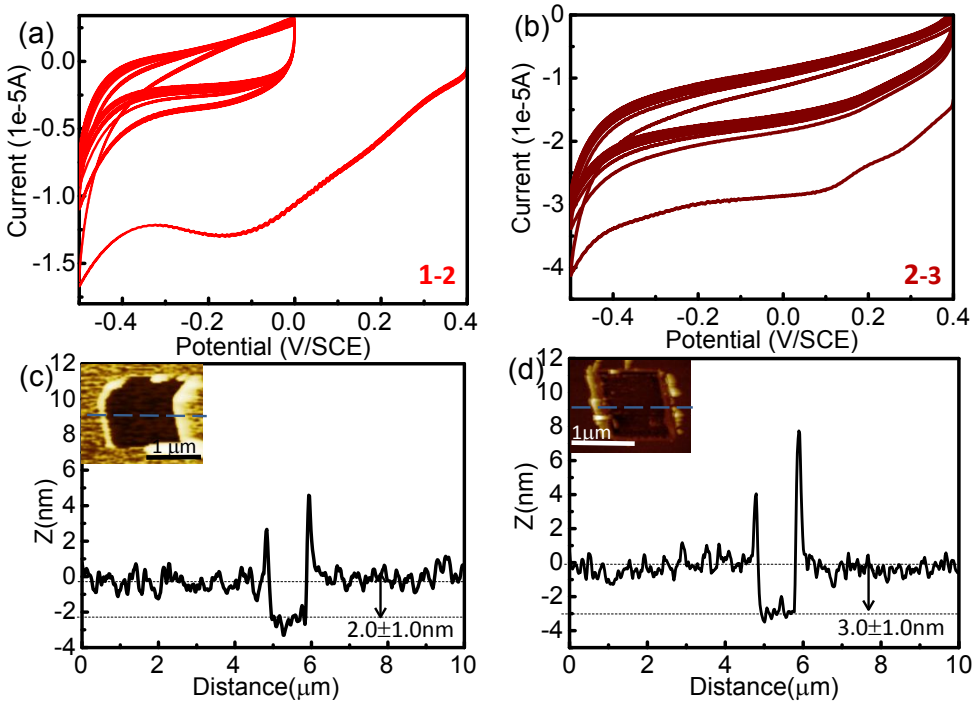

Figure S5. CV of $[Ru(bpy)_3]_n$ electrografting on Au substrate (5×10^{-4} M $Ru(bpy)_3$ with 0.1M $TBAPF_6$ in ACN solution, scan rate 0.1V/S); (a) n=1-2 (b) n=2-3(possible type of oligomers existing on substrates). Thickness characterization by AFM scratch (c) n=1-2 (d) n=2-3.

4. STM-bj results

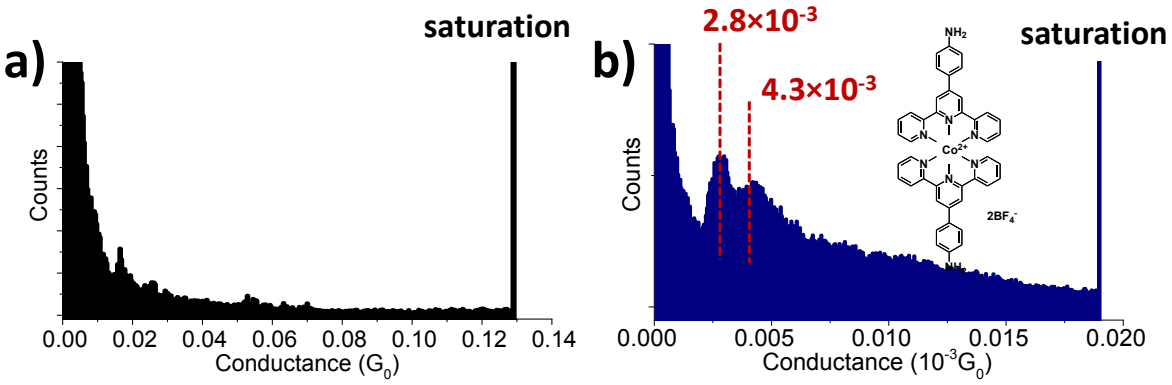

Figure S6. a) Histograms plotted from 300 blank conductance traces showing no conductance peaks. b) histograms plotted from Au-Co(tpy)2-Au SMJ.

Scanning tunneling microscopy break junction (STM-bj) technique is employed to characterize the conductance of single molecular junctions(SMJ) which are described in the main text. STM tip is driven into contact with the Au surface (saturation in Figure S6) and is pulled-out from the substrate. Histogram in Figure S6 a) is a given example where the STM tip is in contact with a bare Au surface (conductivity

saturation is reached due to the limit of current amplifier). There is no molecule connected between the tip and the Au electrode. As a result, the observed histogram show an exponential decay and no current peaks are visible. This histogram is recorded as a blank background to compare with those SMJs with molecules connected between the two electrodes (Figure.3.4 in the main text). Histogram in Figure S6 b) is a given example where the observed histogram shows conductive peaks from the SMJ with $Co(tpy)_2$ molecule trapped between the two electrodes.

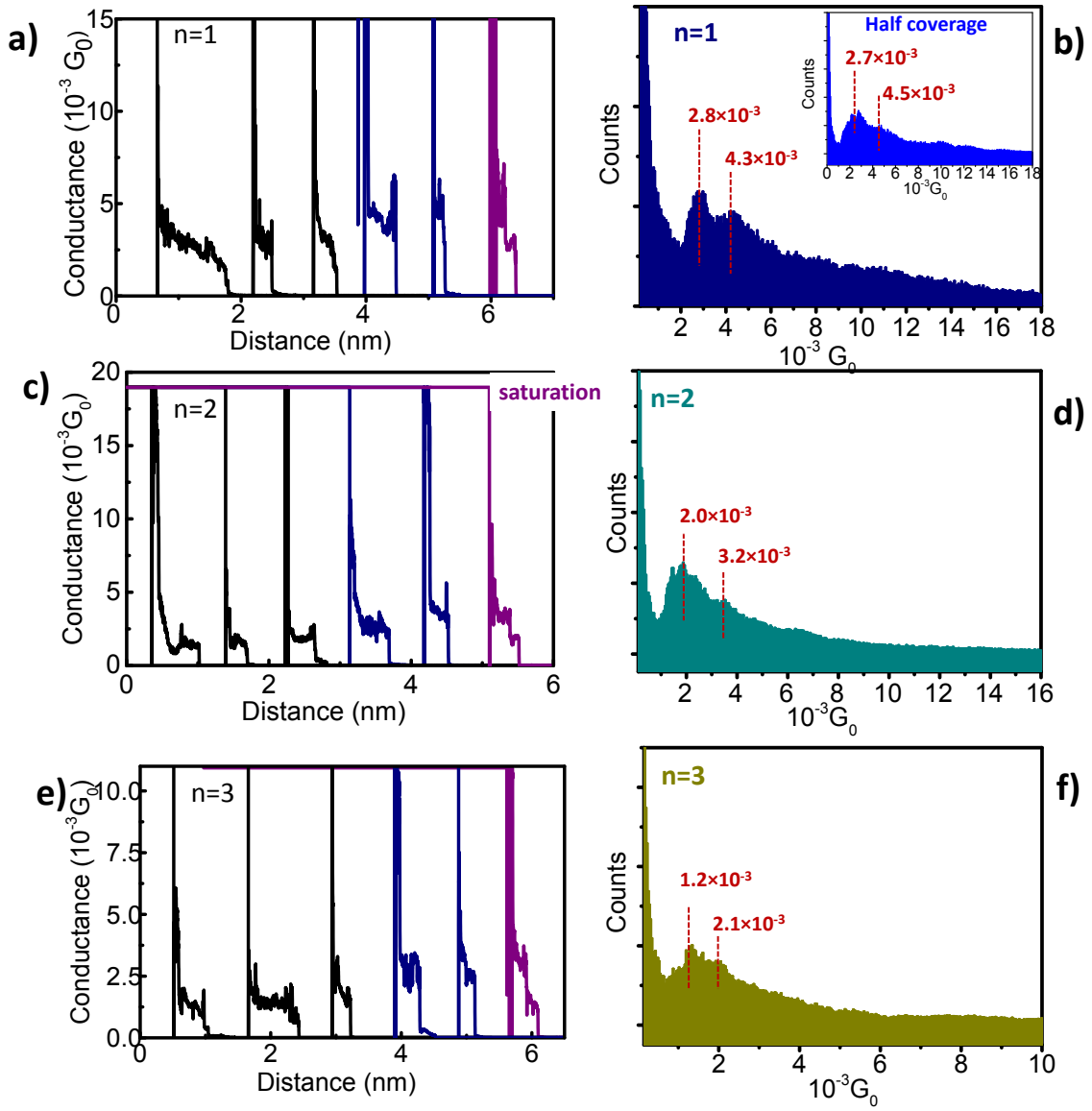

Figure S7. (a) Conductance traces from $[Co(tpy)_2]_1$ SMJs where current plateaus are visible. (a, c, e) Conductance histograms of Au-$[Co(tpy)_2]_n$-Au (n=1,2,3) SMJs are shown in (b, d, f). Inset image in (b) shows a $[Co(tpy)_2]_1$ SMJ histogram measured on a half coverage surface.

The appearance of the current plateaus is a clear signal that molecules are bridged between the two electrodes and that single-molecule junctions are formed. Note that histograms generated with monolayer coverage and submonolayer coverage are identical which indicates that the intermolecular interaction between molecules do not have a large impact on some of the intrinsic transport properties of the junctions. Figure. S7.(a, c e) give a few examples from typical Au-$[Co(tpy)_2]_n$-Au (n= 1, 2 ,3) SMJs where their

conductance-vs-distance (I(d)) traces show current plateaus. The histograms in FigureS7 (b, d, f) are using a linear scale which are different than in the main text using log scale. The current plateaus are with a pulling length range from 5Å up to 1.5 nm which are considered long and stable. The rather long current plateaus (with low noise level) show that our STM-bj technique is giving good signal/noise ratio and the diazoniun grafting formed SMJs possess good stability. Some of the I(d) traces show single current plateaus at two different current values whereas some show double plateaus. The two current plateau values are in corresponding to the LC and HC conductance values observed from the histogram in Figure.S6 (b).

The conductance histograms of Au-$[Co(tpy)_2]_n$-Au (n=1,2,3) SMJs are shown in Figure. S7 (b, d, f), respectively. It is worthwhile to point out that the two SMJs in Figure. S7(b) are single molecule junctions built from a monolayer or a half layer coverage films. The same conductance histograms and the very same conductance values are obtained. This proves that the SMJs can be formed from both a diluted and a densely-packed layers with no influence on the conductance values. All the histograms from Au-$[Co(tpy)_2]_n$-Au are observed showing double peaks due to the split of the low and high conductance which can probably be attributed to the different contact configurations (σ or π electron transfer from nitrogen as described in the main text after Figure3).

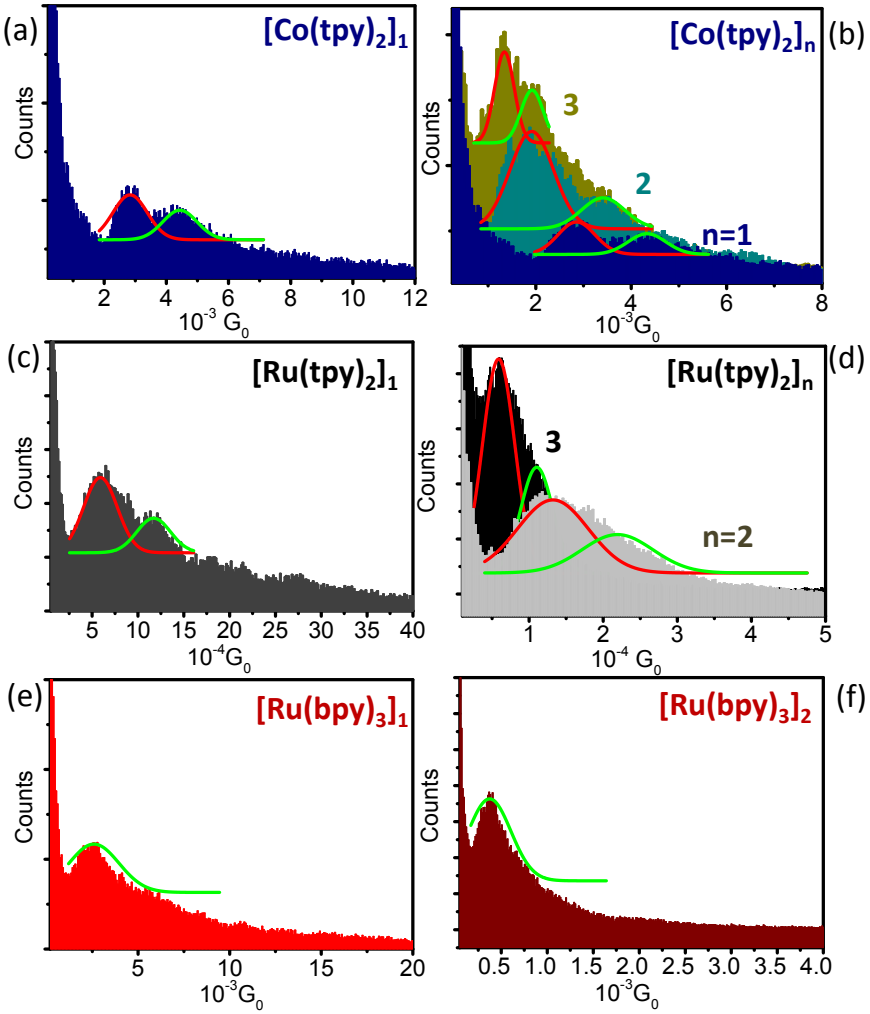

Figure S8. Conductance histograms of $Co(tpy)_2$, $Ru(tpy)_2$ and $Ru(bpy)_3$ based SMJs with Gaussian peak fitting (a,b) Au-$[Co(tpy)_2]_n$-Au SMJs with molecule unit numbers of n=1, 2, 3. (c,d) Au-$[Ru(tpy)_2]_n$-Au SMJs with molecule unit numbers of n=1, 2, 3. (e, f) Au-$[Ru(bpy)_3]_n$-Au SMJs with unit numbers of n=1, 2, respectively.

The conductance histograms from three different molecules $Co(tpy)_2$, $Ru(tpy)_2$ and $Ru(bpy)_3$ grafted with different thickness on Au surface are shown in Figure. S8. Different conductance peaks are observed and they are fitted by Gaussian peaks. The Au-$[Co(tpy)_2]_n$-Au SMJs are investigated with four different samples with the n number vary from one to four. The Au-$Ru[(tpy)_2]_n$-Au SMJs are investigated with two different samples. The first sample is close to have a thickness of monomer, where an Au-$Ru[(tpy)_2]_1$-Au conductance is obtained in Figure S8.c. The second sample is having a thickness around 5±1nm, is therefore a mixed layer of Au-$Ru[(tpy)_2]_2$-Au and Au-$Ru[(tpy)_2]_3$-Au junctions. Two distinct conductance values are obtained at different surface area as shown from the two combined histograms in Figure S8.d. The two SMJs, Au-$Co[(tpy)_2]_n$-Au and Au-$Ru[(tpy)_2]_n$-Au contain the same NH_2 top anchoring groups, are both observed showing double conductance peaks (LC and HC). On the contrary, the Au-$Ru(bpy)_3$-Au SMJs ending with CH top terminal groups, show only single conductance peak. This phenomenon further indicates that the splits of the LC and HC peaks can most probably be attributed from the different electron transfer paths due the different electrode-molecule contact configurations. The ß value is plotted and is calculated using all the conductance values measured in Figure.S8.